

Robust Non-Linear Direct Torque and Flux Control of Adjustable Speed Sensorless PMSM Drive Based on SVM Using a PI Predictive Controller

S. Belkacem*, B. Zegueb and F. Nacéri

Department of Electrical Engineering, University of Batna, 05000, Algeria.

Received 19 October 2009; Revised 24 February 2010; Accepted 20 July 2010

Abstract

This paper presents a new sensorless direct torque control method for voltage inverter – fed PMSM. The control method is used a modified Direct Torque Control scheme with constant inverter switching frequency using Space Vector Modulation (DTC-SVM). The variation of stator and rotor resistance due to changes in temperature or frequency deteriorates the performance of DTC-SVM controller by introducing errors in the estimated flux linkage and the electromagnetic torque. As a result, this approach will not be suitable for high power drives such as those used in tractions, as they require good torque control performance at considerably lower frequency. A novel stator resistance estimator is proposed. The estimation method is implemented using the Extended Kalman Filter. Finally extensive simulation results are presented to validate the proposed technique. The system is tested at different speeds and a very satisfactory performance has been achieved.

Keywords: DTC, SVM, (PMSM), Extended Kalman Filter (EKF), Sensorless.

1. Introduction

Permanent magnet (PM) synchronous motors are widely used in high-performance drives such as industrial robots and machine tools. These motors have many advantages as: high efficiency and power density, high-torque/inertia ratio. The fast development of power-and microelectronics and computer science opened a new way of investigation for PMSM with vector control strategies [1, 2]. Firstly DTC was proposed for IM [3], however now is applied also for PMSM [4]. Direct Torque Control (DTC) seems to be a good performance alternative to the classical vector control drives. After its implementation on induction motor drives, this control method in recent years has been proposed for permanent magnet synchronous motor with good results. DTC is able to produce fast torque and stator flux response with a well designed flux, torque and speed estimator. In order to reduce the torque and current pulsations, in steady state a mixed DTC- SVM control method seems more suitable.

SVM techniques [5, 6] offer better DC link utilization and they lower the torque ripple. The emphasis of research on PMSM has been on sensorless drive [7, 8, 9, 10], which eliminates flux and speed sensors mounted on the motor. In addition, the development of effective speed and flux estimators has allowed good rotor flux-oriented performance at all speeds except those close to zero. Sensorless control has improved the motor performance, compared to the Volts/Hertz (or constant flux) controls.

The EKF is considered to be suitable for use in high-perform-

ance PMSM drives, and it can provide accurate speed estimates in a wide speed-range, including very low speed [11, 12].

The variation of stator resistance due to changes in temperature or frequency deteriorates the performance of DTC controller by introducing errors in the estimated flux linkage and the electromagnetic torque [13, 14, 15, 16]. A novel stator resistance estimator during the operation of the motor is proposed.

This paper describes a novel DTC-SVM method for a speed sensorless control of PMSM drive. According to this method, a conventional PI predictive controller is used to determine the polar components of the voltage command vector. The results show that a satisfactory control performance is obtained.

2. Modeling of the PMSM

The electrical and mechanical equations of the PMSM in the rotor reference (d,q) frame as follows:

$$\begin{cases} \frac{dI_d}{dt} = -\frac{R_s}{L_d} + \frac{L_q}{L_d} P\omega_r I_q + \frac{1}{L_d} U_d \\ \frac{dI_q}{dt} = -\frac{R_s}{L_q} - \frac{L_d}{L_q} P\omega_r I_d - \frac{\Phi_f}{L_q} P\omega_r + \frac{1}{L_q} U_q \\ \frac{d\omega_r}{dt} = \frac{3P}{2J} [(L_d - L_q) I_q I_d + \Phi_f I_q] - \frac{1}{J} T_L - \frac{B}{J} \omega_r \end{cases} \quad (1)$$

* E-mail address: Belkacem_sebti@yahoo.fr

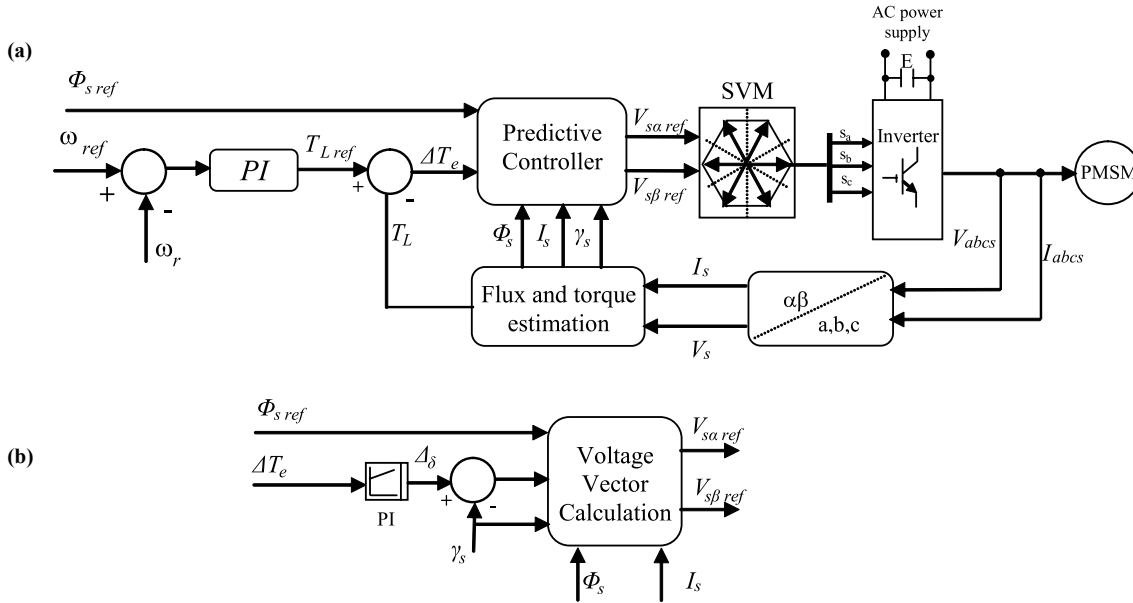


Figure 1. (a) Induction Motor Drive System Control. (b) PI Predictive Controller.

where I_d, I_q are the $d-q$ axis currents, U_d, U_q are the $d-q$ axis voltages, ω_r denotes the rotor speed, R_s is the stator resistance, L_d, L_q are the stator inductances, P is the pole pairs, J is the rotor moment of inertia, B is the viscous friction coefficient, T_L is the load torque.

The block scheme of the investigated direct torque control with space vector modulation (DTC-SVM) for a voltage source PWM inverter fed PMSM is presented in Figure 1(a).

The internal structure of the predictive torque and flux controller is shown in Figure 1(b).

The objective of the DTC-SVM scheme, and the main difference between the classic DTC, is to estimate a reference stator voltage vector $V_{s\ ref}$ in order to drive the power gates of the inverter with a constant switching frequency. Although, the basic principle of the DTC is that the electromagnetic torque of the motor can be adjusted by controlling the angle $\Delta\delta$ between the stator and rotor flux vectors, the torque of a PMSM can be calculated by the following equation.

$$T_L = \frac{3}{2} P \frac{\Phi_{s\ ref}}{L_d L_q} \left[\Phi_f L_q \sin(\delta) + \frac{1}{2} \Phi_{s\ ref} (L_d - L_q) \sin(2\delta) \right] \quad (2)$$

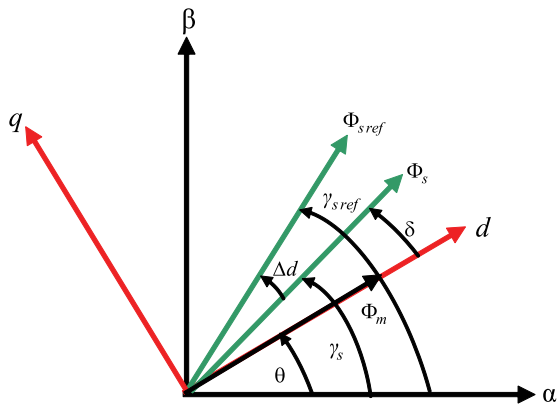


Figure 2. Vector Diagram of Illustrating Torque Control.

The change in torque can be given by the following formulation,

$$\Delta T_L = 3 \left(\frac{p}{2} \right) \frac{|\Phi_f| |\Phi_s + \Delta\Phi_s| \sin\delta}{L_d} \quad (3)$$

Where the change in the stator flux vector, if we neglect the voltage drop in the stator resistance, can be given by the following equation,

$$\Delta\Phi_s = V_s T_s \quad (4)$$

Where $\Delta\Phi_s$ is the deviation from $|\Phi_s|$ which are defined by:

$$\Delta\Phi_s = \left| \Phi_{s\ ref} \right| - \left| \Phi_s \right| \quad (5)$$

The predictive controller determines the stator voltage command vector in polar coordinates $V_{s\ ref} [V_{s\ ref}, \delta]$ for space vector modulator; which finally generates the pulses S_a, S_b, S_c .

Sampled torque error ΔT_e and reference stator flux amplitude $\Phi_{s\ ref}$ are delivered to the predictive controller. The relation between error of torque and increment of load and angle $\Delta\delta$ is nonlinear. Therefore PI controller, which generates the load angle increment required to minimize the instantaneous error between reference T_{ref} and actual T_e torque, has been applied. The reference values of the stator voltage $V_{s\ ref}, \gamma_{s\ ref}$ is calculated based on stator resistance $R_s, \Delta\delta$ signal, actual stator current vector I_s , actual stator flux amplitude Φ_s and position γ_s as: The α, β axes components of the stator reference voltage $V_{s\ ref}$, are calculated according to the following equation:

$$V_{sa\ ref} = \frac{\Phi_{s\ ref} \cos(\gamma_s + \Delta\delta) - \Phi_{s\ ref} \cos(\gamma_s)}{T_s} + \hat{R}_s I_{sa} \quad (6)$$

$$V_{sb\ ref} = \frac{\Phi_{s\ ref} \sin(\gamma_s + \Delta\delta) - \Phi_{s\ ref} \sin(\gamma_s)}{T_s} + \hat{R}_s I_{sb} \quad (7)$$

$$V_{s\text{ref}} = \sqrt{V_{s\alpha\text{ref}}^2 + V_{s\beta\text{ref}}^2} \quad (8)$$

$$\gamma_{s\text{ref}} = \arctan\left(\frac{V_{s\beta\text{ref}}}{V_{s\alpha\text{ref}}}\right) \quad (9)$$

Where, T_s is sampling time.

3. Voltage Space Vector Modulation

The voltage vectors, produced by a 3-phase PWM inverter, divide the space vector plane into six sectors as shown in Figure 3.

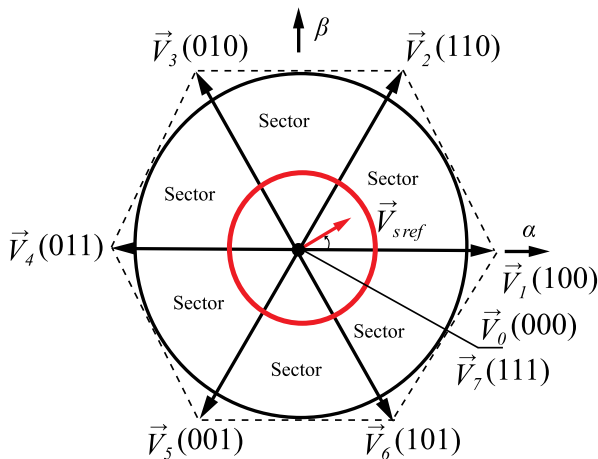


Figure 3. The Diagram of Voltage Space Vectors.

In every sector, each voltage vector is synthesized by basic space voltage vector of the two side of sector and one zero vector. For example, in the first sector, $V_{s\text{ref}}$ is a synthesized voltage space vector and expressed by:

$$V_{s\text{ref}} T_s = V_0 T_0 + V_1 T_1 + V_2 T_2 \quad (10)$$

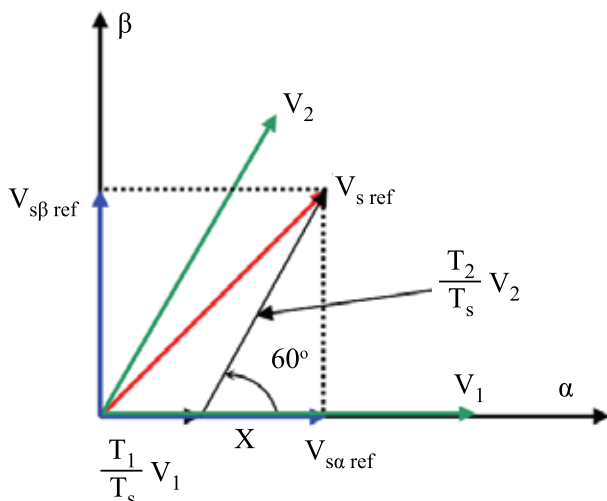


Figure 4. Projection of the Reference Voltage Vector.

$$T_s = T_0 + T_1 + T_2 \quad (11)$$

Where T_0 , T_1 and T_2 is the work time of basic space voltage vectors V_0 , V_1 and V_2 respectively.

The determination of the amount of times T_1 and T_2 is given by simple projections:

$$T_1 = \frac{T_s}{2E} (\sqrt{6} \cdot V_{s\beta\text{ref}} - \sqrt{2} \cdot V_{s\alpha\text{ref}}) \quad (12)$$

$$T_2 = \sqrt{2} \frac{T_s}{E} V_{s\beta\text{ref}} \quad (13)$$

The rest of the period spent in applying the null-vector. For every sector, commutation duration is calculated. The amount of times of vector application can all be related to the following variables:

$$X = \frac{T_s}{E} \sqrt{2} \cdot V_{s\beta\text{ref}} \quad (14)$$

$$Y = \frac{T_s}{E} \left(\frac{\sqrt{2}}{2} \cdot V_{s\beta\text{ref}} + \frac{\sqrt{6}}{2} \cdot V_{s\alpha\text{ref}} \right) \quad (15)$$

$$Z = \frac{T_s}{E} \left(\frac{\sqrt{2}}{2} \cdot V_{s\beta\text{ref}} - \frac{\sqrt{6}}{2} \cdot V_{s\alpha\text{ref}} \right) \quad (16)$$

The application durations of the sector boundary vectors are tabulated as follows:

Table 1. Durations of the sector boundary vectors.

SECTOR	1	2	3	4	5	6
T_1	Z	Y	-Z	-X	X	-Y
T_2	Y	-X	X	Z	-Y	-Z

The goal of this step is to compute the three necessary duty cycles as;

$$T_{aon} = \frac{T_s - T_1 - T_2}{2} \quad (17)$$

$$T_{bon} = T_{aon} + T_1 \quad (18)$$

$$T_{con} = T_{bon} + T_2 \quad (19)$$

The last step is to assign the right duty cycle (T_{aon}) to the right motor phase according to the sector.

Table 2. Assigned duty cycles to the PWM outputs.

SECTOR	1	2	3	4	5	6
S _a	T _{bon}	T _{aon}	T _{aon}	T _{con}	T _{bon}	T _{con}
S _b	T _{aon}	T _{con}	T _{bon}	T _{bon}	T _{con}	T _{aon}
S _c	T _{con}	T _{bon}	T _{con}	T _{aon}	T _{aon}	T _{bon}

4. Extended Mathematical Model of the PMSM

In this study, EKF, is used for the estimation of I_d, I_q, ω_r, δ, T_r and \hat{R}_s .

Figure 5 shows the structure of a Kalman filter

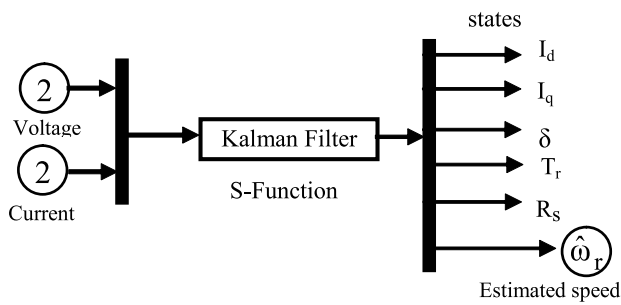


Figure 5. Simulink Model of EKF Speed Estimation.

The discrete model of the PMSM can be given as follows:

$$x(k+1) = f(x(k), u(k)) + W(k) = A_d x(k) + B_d U(k) + W(k) \quad (20)$$

$$y(k) = h(x(k)) + V(k) = C_d x(k) + V(k)$$

With: w(k) is the measurement noise and v(k): is the process noise, A_d, B_d and C_d matrix of discrete system.

$$A_d = e^{AT_s} \approx I - AT_s$$

$$B_d = \int_0^{T_s} e^{A\tau} B d\tau \approx BT_s \quad (21)$$

$$C_d = C$$

I: identity matrix of system depending on the size of the state vector.

$$x = [I_d \quad I_q \quad \omega_r \quad \delta \quad T_r \quad R_s]^T$$

$$u = [u_d \quad u_q]^T \quad y = [I_d \quad I_q]^T$$

$$f[x(k), u(k)] = \begin{bmatrix} f_1 \\ f_2 \\ f_3 \\ f_4 \\ f_5 \\ f_6 \end{bmatrix} \quad (22)$$

Where:

$$f_1 = (1 - a_1 R_s(k)) I_d(k) + a_2 \omega_r(k) I_q(k) + a_3 u_d(k)$$

$$f_2 = a_4 \omega_r(k) I_d(k) + (1 - a_5 R_s(k)) I_q(k) - a_6 \omega_r(k) + a_7 u_q(k)$$

$$f_3 = a_8 I_d(k) I_q(k) + a_9 I_q(k) + (1 - a_{10}) \omega_r(k) + a_{11} T_r(k)$$

$$f_4 = a_{12} \omega_r(k) + \delta(k)$$

$$f_5 = T_r(k)$$

$$f_6 = R_s(k)$$

$$A_d = \begin{bmatrix} (1 - a_1 R_s(k)) & a_2 \omega_r(k) & 0 & 0 & 0 & a_1 \\ -a_4 \omega_r(k) & (1 - a_5 R_s(k)) & -a_6 & 0 & 0 & a_5 \\ a_8 I_q(k) & a_9 & 1 - a_{10} & 0 & a_{11} & 0 \\ 0 & 0 & a_{12} & 1 & 0 & 0 \\ 0 & 0 & 0 & 0 & 1 & 0 \\ 0 & 0 & 0 & 0 & 0 & 1 \end{bmatrix} \quad (23)$$

$$B_d = \begin{bmatrix} a_3 & 0 & 0 & 0 & 0 & 0 \\ 0 & a_7 & 0 & 0 & 0 & 0 \end{bmatrix}^T$$

$$C_d = \begin{bmatrix} 1 & 0 & 0 & 0 & 0 & 0 \\ 0 & 1 & 0 & 0 & 0 & 0 \end{bmatrix}^T$$

$$a_1 = \frac{R_s}{L_d} T_s; \quad a_2 = \frac{L_q}{L_d} T_s; \quad a_3 = \frac{1}{L_d} T_s$$

$$a_4 = \frac{L_d}{L_q} T_s; \quad a_5 = \frac{R_s}{L_q} T_s; \quad a_6 = \frac{\Phi_f}{L_q} T_s$$

$$a_7 = \frac{1}{L_q} T_s; \quad a_8 = p \frac{L_d - L_q}{J} T_s; \quad a_9 = p \frac{\Phi_f}{J} T_s$$

$$a_{10} = \frac{B}{J} T_s; \quad a_{11} = \frac{1}{J} T_s; \quad a_{12} = p T_s$$

Where: f(x(k), u(k)): Nonlinear function vector of the states. x(k): extended state vector. A_d: system matrix. u_e(k) is the control input vector, B_d: input matrix. h(x(k), v(k)): Function vector of the outputs. C_d: Measurement matrix. w(k) and v(k): process and measurement noise respectively.

5. Application of the Extended Kalman Filter

The speed estimation algorithm of the extended Kalman filter can be simulated by the MATLAB/Simulink software, which consists of an S-Function block as shown in Figure 5.

5.1. Prediction of the State Vector

Prediction of the state vector at sampling time (k+1), from the input u (k), state vector at previous sampling time x(k/k).

$$\hat{x}(k + 1/k) \hat{=} f(\hat{x}(k/k), u(k)) \tag{24}$$

5.2. Prediction Covariance Computation

The prediction covariance is updated by:

$$P(k + 1/k) = f(k)P(k)F(k)^T + Q \tag{25}$$

Where: Q: covariance matrix of the system noise,

$$F(k) = \left. \frac{\partial f}{\partial x} \right|_{x(k)=\hat{x}(k/k)} \tag{26}$$

5.3. Kalman Gain Computation

The Kalman filter gain (correction matrix) is computed as;

$$L(k + 1) = P(k + 1/k)C(k)^T (C(k)P(k + 1/k)C(k)^T + R)^{-1}$$

With: $C(k) = \left. \frac{\partial c(x(k))}{\partial x(k)} \right|_{x(k)=\hat{x}(k)}$ (27)

5.4. State Vector Estimation

The predicted state-vector is added to the innovation term multiplied by Kalman gain to compute state-estimation vector. The state-vector estimation (filtering) at time (k) is determined as:

$$\hat{x}(k + 1/k + 1) = \hat{x}(k + 1/k) + L(k + 1)(y(k + 1) - C\hat{x}(k + 1/k)) \tag{28}$$

6. Proposed Sensorless PMSM Drive

The proposed sensorless PMSM drive is depicted in Figure 6. The stator flux is estimated by the EKF and used in the DTC control

the parameters are listed in Table 3.

Table 3. Durations of the sector boundary vectors.

Parameters of the PMSM	
Rated torque	5 Nm
d-Axis inductance	$L_d = 0.0066$ H
q-Axis inductance	$L_q = 0.0058$ H
Stator resistance	$R_s = 1.4$
Moment of rotor inertia	$J = 0.00176$ kgm ²
Magnetic flux linkage	$\Phi_f = 0.1546$ Wb
Viscous friction coefficient	$f = 0.00038$ Kg.m ² /s
Numbers of pole pairs	$P = 3$

7. Simulation Results

In this section, the effectiveness of the proposed algorithm is verified by computer simulations. During the simulations, the torque set value is limited to 5 N.m (rated torque), In order to show the performances and the robustness of the combined DTC-SVM-EKF algorithm, a series of tests were conducted to check the performance of the proposed DTC-SVM. In all sketched figures, the time axis is scaled in seconds. The block scheme of the investigated direct torque control with space vector modulation (DTC-SVM) for a voltage source inverter fed PMSM is presented in (Figure 6).

The specifications for the used PMSM are listed in table (3).

Figure 7 shows the actual and estimated responses of the proposed sensorless scheme. The machine is started from rest and assumed to follow a certain speed trajectory. A load torque of 5 N.m. is assumed to be applied at time 0.15s. Current ripple has also a notable reduction in DTC-SVM compared to classic DTC.

DTC-SVM has a significantly lower ripple level both in torque, flux and stator current, a lower current ripple advantageous because the machine will have less EMI noise.

Figure 8 show the trajectory of the estimated stator flux components DTC-SVM has as good dynamic response as the classical DTC.

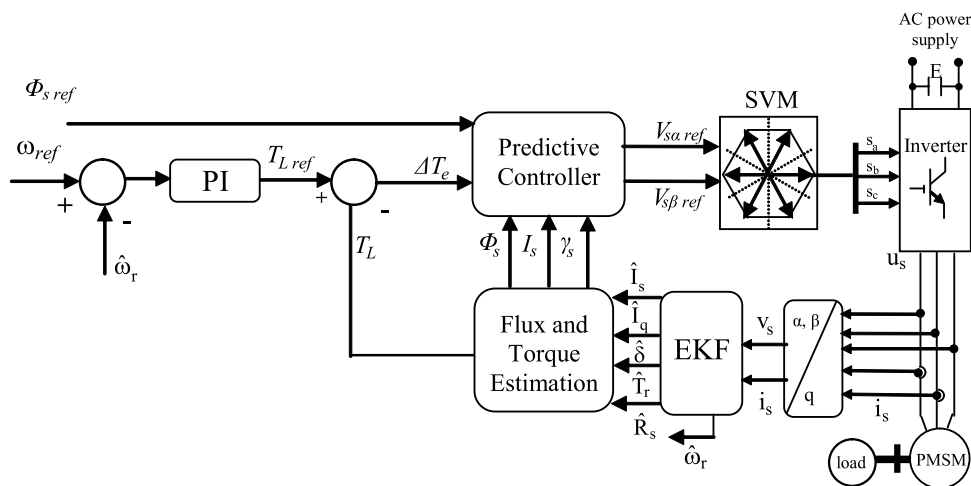


Figure 6. Block diagram of the sensorless system.

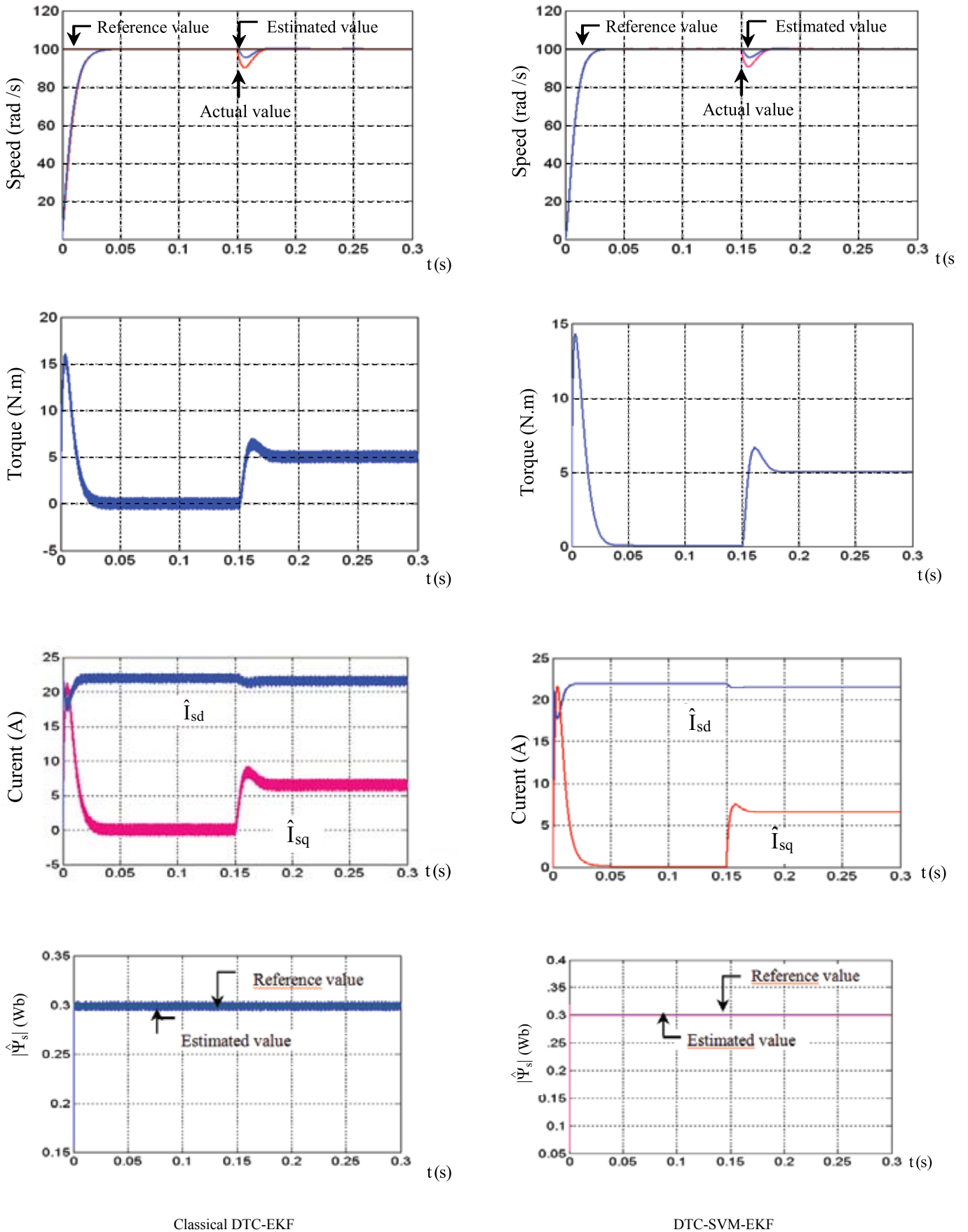


Figure 7. Simulation results: A load torque of 5 'N.m) is applied at t = 0.15 sec.

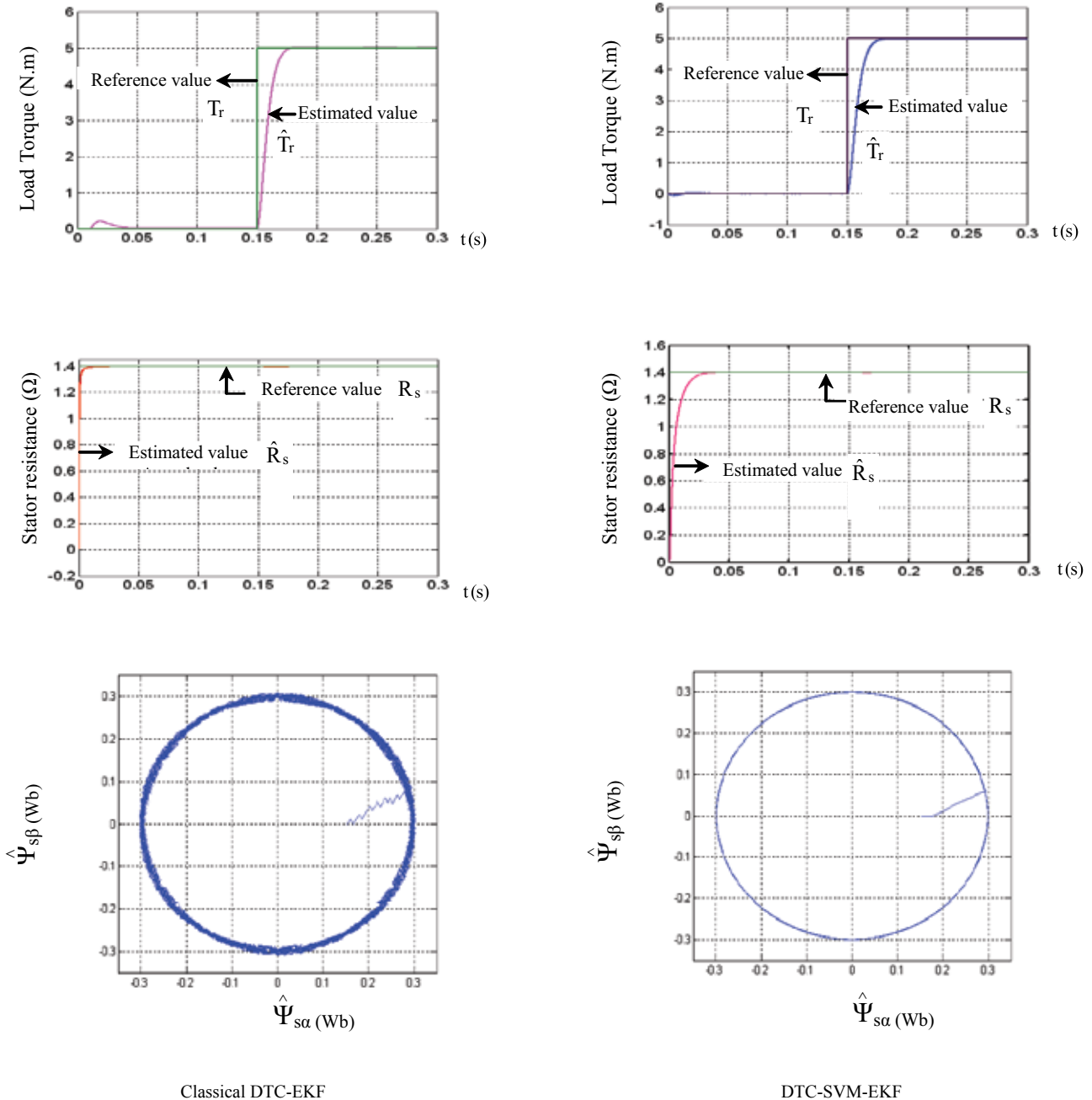


Figure 8. Simulation results

8. Conclusion

In this paper an extended Kalman filter (EKF) algorithm is developed for the speed sensorless direct torque control strategy combined with space vector modulation. The complete sensorless solution is presented with the combined DTC-SVM-EKF strategy; low torque ripple operation has been obtained with PMSM. In spite of lower switching frequency, the DTC-SVM scheme has lower harmonic current, and consequently lower ripple than conventional hysteresis based DTC. Simulation results obtained clearly demonstrate the effectiveness of the estimator in estimat-

ing the stator resistance and improving performance of DTC. Additionally, the application of SVM guarantee:

- Inverter switching frequency is constant;
- Distortion caused by sector changes is delimited;
- Low sampling frequency is required;
- High robustness;
- Good dynamic response;
- Low complexity.

References

1. I. Takahashi and T. Noguchi, A new quick-response and high efficiency control strategy of an induction machine, *IEEE Trans. Industry Appl*, Vol. 22, pp. 820-827 (Sep/Oct 1986).
2. A. Goed, I. da Silva and P. Jose, A. Serni, A hybrid controller for the speed control of a permanent magnet synchronous motor drive, *Control Engineering Practice*, Vol. 16, Issue 3, pp. 260-270 (March 2008).
3. T. Vyncke, K. Boel and A. Melkebeek, direct torque control of permanent magnet synchronous motors – an overview, *IEEE symposium in electrical power engineering, Belgium* (27-28 April 2006).
4. B. Akin A , State Estimation Techniques for Speed Sensorless Field Oriented Control of induction Motor, Thesis submitted to the graduate school of the middle east technical university (August 2003).
5. Z. Hilmi Bin Ismail, Direct torque control of induction motor drives using space vector modulation (DTC-SVM), Master of Engineering Faculty of Electrical Engineering Malaysia (November, 2005).
6. M. P. Kazmierkowski, M. Zelechowski, D. Swierczynski, Simple DTC-SVM Control Scheme for Induction and PM Synchronous Motor, XVII International Conference on Electrical Machines, IECM 2006, Chania (September 2-5, 2006).
7. S. Baris Ozturk, Modelling, simulation and analysis of low-cost direct torque control of PMSM using hall-effect sensors, Master of Science, Texas University (December 2007).
8. A. Paladugu, H. Chowdhury, Sensorless control of inverter-fed induction motor drives, *Electric Power Systems Research*, Vol. 77, Issues 5-6, pp. 619-629 (April 2007).
9. C. Bian Shuangyan, R. Liangyu, Sensorless “DTC of Super High-speed PMSM, Proceedings of the IEEE International Conference on Automation and Logistics, Jinan, China (18 - 21 August 2007).
10. S. Benagoune, S. Belkacem and R. Abdessemed, Sensorless direct torque control of PMSM drive with EKF estimation of speed, rotor position and load torque observer, *Al-Azhar University Engineering Journal, JAUES, Egypt*, Vol. 2, No. 5, pp.469-479 (Apr. 2007).
11. M. Barut, S. Bogosyan and M. Gokasan, Switching EKF technique for rotor and stator resistance estimation in speed sensorless control of IMs *Energy Conversion and Management*, Vol. 48, Issue 12, pp. 3120-3134 (December 2007).
12. M. Kosaka and H. Uda, Sensorless IPMSM drive with EKF estimation of speed and rotor position, *Journal of low frequency noise, vibration and active control*, Vol. 22, No. 4, pp. 59-70 (2004).
13. M. Kadjoudj, N. Goléa and M. E. H Benbouzid, Problems of Stator Flux Estimation in DTC of PMSM Drives, *Journal of Electrical Engineering & Technology*, Vol. 2, No. 4, pp. 468-477 (2007).
14. M. E. Haque and M. F. Rahman, Influence of stator resistance variation on direct torque controlled interior permanent magnet synchronous motor drive performance and its compensation, *IEEE Industry Application Society Annual Meeting, Chicago, USA*, Vol. 4, pp. 2563-2569 (2001).
15. Yanping Xu, Yanru Zhong, Jie Li, Fuzzy Stator Resistance Estimator for a Direct Torque Controlled Interior Permanent Magnet Synchronous Motor, *ICEMS 2005. Proceedings of the 8th International Conference on Electrical Machines and Systems*, pp.438-441, (27-29 Sept. 2005).
16. C. Yongjun, H. Shenghua, W. Shanming, W. Fang, Direct Torque Controlled Permanent Magnetic Synchronous Motor System Based on the New Rotor Position Estimation, *Proceedings of the 26th Chinese Control Conference, Zhangjiajie, Hunan, China*, (26-31 July 2007).